Journal of Theoretical Biology 285 (2011) 58–68

Contents lists available at ScienceDirect

Journal of Theoretical Biology

journal homepage: www.elsevier.com/locate/yjtbi

Adaptive diversification of a plastic trait in a predictably fluctuating environment

Matthew D. Herron*, Michael Doebeli

Department of Zoology, University of British Columbia, #2370–6270 University Boulevard, Vancouver, B.C., Canada V6T 1Z4

ARTICLE INFO

Article history:
Received 16 March 2011
Received in revised form
2 June 2011
Accepted 7 June 2011
Available online 28 June 2011

Keywords:
Adaptive dynamics
Escherichia coli
Genetic assimilation
Metabolism
Phenotypic plasticity

ABSTRACT

There is substantial evidence that evolutionary diversification can occur in allopatric conditions through reduction in the degree of phenotypic plasticity when an isolated population encounters a novel, more stable environment. Plasticity is no longer favored in the new environment, either because it carries an inherent physiological cost or because it leads to production of suboptimal phenotypes. In order to explore the role of phenotypic plasticity in sympatric diversification, we modeled the ecological and evolutionary dynamics of *Escherichia coli* bacteria in batch cultures. Our results describe an evolutionary pathway leading to metabolic diversification in a sympatric environment without spatial structure. In an environment that fluctuates widely and predictably, evolutionary branching leads to diversification and stable coexistence of generalist and specialist ecotypes for some combinations of parameters. Diversification and stable coexistence occur when reaction norms are steep and trade-offs between metabolic pathways are convex. We conclude that, in principle, diversification due to reduced plasticity can occur without allopatric isolation, reduced environmental variability, or an explicit cost of plasticity.

1. Introduction

The role of phenotypic plasticity in evolutionary diversification (and in evolution more generally) is the subject of ongoing debate. Recent assessments range from "phenotypic plasticity as a major mechanism for evolution…has, at present, neither empirical nor model support" (de Jong, 2005, p. 101) to "recent theory and data implicate phenotypic plasticity as playing a key role in promoting diversification…" (Pfennig et al., 2010, p. 465).

Several comparative studies have provided indirect evidence of a role of phenotypic plasticity in diversification, generally by showing that extant species have genetically fixed phenotypic differences similar to those that can be induced plastically in an ancestor (Pfennig et al., 2010). For example, in island populations of tiger snakes (*Notechis scutatus*), common garden experiments showed that young island populations (those recently derived from mainland populations) achieve large head size through phenotypic plasticity, while older island populations are genetically fixed for a similar phenotype (Aubret and Shine, 2009). In three-spined sticklebacks, plasticity in both morphology and osmoregulation in the (presumed ancestral) marine population is substantially reduced in at least some of the (derived) freshwater forms (McCairns and Bernatchez, 2010; Wund et al., 2008).

In each of these cases, a reduction in plasticity is thought to have resulted from an isolated population encountering a novel, more stable environment. Plasticity is no longer favored, either because it carries an inherent physiological cost or because it leads to production of suboptimal phenotypes. Here, we show that diversification due to reduced plasticity can occur without allopatric isolation, reduced environmental variability, or an explicit cost of plasticity.

Our model is based on a series of experiments by Doebeli and colleagues (Friesen et al., 2004; Le Gac et al., 2008; Spencer et al., 2007; Spencer et al., 2008; Tyerman et al., 2005), in which *Escherichia coli* bacteria grown in batch culture consistently diversified into two genetically distinct ecotypes that differ in their relative growth rates on glucose and acetate. The "large" or slow-switcher (SS) strains have higher growth rates on glucose but switch more slowly to acetate metabolism than the "small" or fast-switcher (FS) strains ("large" and "small" refer to the size of colonies grown on agar plates). Slow switchers also exhibit lower maximum growth rates than fast switchers when glucose is exhausted and acetate metabolism becomes the primary source of energy. Relative to a more plastic ancestor, SS strains are glucose specialists, which upregulate the glycolysis/pyruvate decarboxylation pathway (hereafter referred to simply as glycolysis) at the expense of acetate assimilation and the tricarboxylic

* Corresponding author.
E-mail address: xprinceps@gmail.com (M.D. Herron).

0022-5193/$ - see front matter © 2011 Elsevier Ltd. All rights reserved.
doi:10.1016/j.jtbi.2011.06.007

acid (TCA) cycle (Le Gac et al., 2008). The FS strains are generalists capable of growth on glucose or acetate. Relative to the ancestor, FS strains upregulate acetate assimilation and the TCA cycle at the expense of glucose catabolism (Le Gac et al., 2008).

E. coli grown in a mixture of glucose and acetate preferentially consume the glucose first, switching to acetate catabolism only when the glucose is exhausted. Metabolism is thus plastic with respect to the extracellular concentration of glucose: when glucose concentration is high, glucose is converted into energy through glycolysis, resulting in production of acetate, which is excreted from the cell as a waste product. When glucose drops below a threshold concentration, the acetate uptake and oxidative respiration pathways become active, and acetate is reduced to CO_2 through the TCA cycle. The resulting two-phase growth curves, characterized by rapid early growth and slower growth following glucose depletion, are known as diauxic.

Catabolic pathways are subject to a trade-off between the rate of ATP production and the yield of ATP per molecule of substrate (Gudelj et al., 2007; Novak et al., 2006), which constrains pathways to a spectrum from fast but inefficient to efficient but slow. The combination of glycolysis and acetate excretion is nearer the fast/inefficient end of the spectrum, producing ATP quickly but gaining only a few ATP molecules per molecule of substrate, while acetate uptake and oxidative respiration produce a much larger number of ATP molecules per molecule of substrate but do so more slowly.

In the experiments of Doebeli and colleagues, the early phase of evolution was characterized by a directional change, specifically a reduction in the lag time between growth on glucose and growth on acetate (Spencer et al., 2008). This directional change was followed by diversification into the two recognizably distinct metabolic types: one (FS) that begins exploiting acetate earlier in the 24 h growth cycle and grows relatively quickly after glucose is exhausted and one (SS) that grows more quickly early in the growth cycle (when glucose is abundant) but that is unable to efficiently switch to acetate catabolism after glucose is depleted (Le Gac et al., 2008; Tyerman et al., 2008).

Genetic changes occurred both in the early, directional phase of the experiment (distinguishing both derived types from the ancestral strain) and after diversification (distinguishing FS from SS) (Le Gac et al., 2008). Phenotypically, though, the SS type is similar to the ancestral strain, while the FS type represents a novel metabolic strategy (Spencer et al., 2008; Tyerman et al., 2008).

FS and SS types can coexist on ecological timescales in a homogeneous, well-mixed environment (Friesen et al., 2004; Tyerman et al., 2005). Invasion experiments in which the two types were mixed in various initial proportions consistently stabilized at intermediate frequencies, suggesting that diversification and coexistence resulted from negative frequency-dependent selection (Friesen et al., 2004; Tyerman et al., 2005).

In order to explore the role of phenotypic plasticity in sympatric diversification, we modeled the ecological and evolutionary dynamics of *E. coli* in batch cultures. Bacterial metabolism was represented as a system of differential equations representing the kinetics of the central metabolic pathways using Michaelis–Menten equations. Bacterial population growth, environmental feedbacks, and evolutionary dynamics emerged from the metabolic activity of individual bacteria. We used the resulting model to explore the conditions in which changes in phenotypic plasticity can lead to metabolic diversification in a well-mixed, sympatric population.

The fundamental assumption of our model is that a trade-off exists between the expression of (1) the enzymes involved in glycolysis and acetate excretion and (2) those involved in acetate uptake and oxidative respiration. These expression levels are the plastic traits of our interest, and the reaction norms in our model describe their responses to the concentration of nutrients (glucose) available in the medium. Since we further assume that the rates of these pathways are proportional to their expression levels, the trade-off in expression amounts to a trade-off between the rates of the respective pathways.

The evolutionary dynamics of this system were previously modeled by Friesen et al. (2004); the current model differs from the previous model in several important respects. First, we exploit the detailed understanding of the *E. coli* central metabolic pathways to model the metabolism of individual bacteria in terms of explicit enzyme kinetics. In addition, we model metabolic reaction norms as continuous functions, rather than as a switching function in which a given pathway is either fully "on" (expressed at its maximum level) or fully "off" (not utilized). Finally, we do not assume that the trade-off between growth on glucose and growth on acetate is linear; rather we treat the shape of the trade-off curve as a parameter and explore concave, linear, and convex trade-offs. Trade-off curvature has been shown to be an important factor in diversification in adaptive dynamics models (e.g. Doebeli, 2002; Kisdi, 2001), and the shape of the trade-off curve turns out to have a strong influence on evolutionary outcomes in our model as well.

2. Model

The basic structure of our model is as follows. In Section 2.1, we derive an ecological model describing the dynamics of a bacterial population and of the composition of the growth medium during a single batch culture of 24 h. The model is based on the stoichiometry and kinetics of *E. coli* metabolism, and it reflects a feedback in which bacterial growth both affects and is affected by the growth environment. The ecological model thus describes both the growth dynamics of the bacterial population and the dynamics of the medium, i.e., the environment. Given the relevant stoichiometric and metabolic parameters, the behavior of the ecological model is determined by the phenotypic properties of the bacteria in the batch culture, specifically, the expression levels of metabolic enzymes. In Section 2.2, we derive an evolutionary model, based on the ecological model in Section 2.1, describing the evolution of traits determining metabolic enzyme expression. Through their effects on bacterial metabolism and growth, these traits determine the ecological environment (i.e., temporal changes in substrate concentrations) that mutant phenotypes experience, and hence determine the selection environment for mutants. This then sets the stage for an adaptive dynamics analysis.

2.1. Ecological model

To build the model, we first described *E. coli* metabolism by assuming that the kinetics of each pathway could be represented as a single reaction using Michaelis–Menten dynamics. This simplifying assumption has been used in several similar models and yielded results that are biologically realistic (e.g., Gudelj et al., 2007; Pfeiffer and Bonhoeffer, 2004). Stoichiometry of *E. coli* central metabolism was based on that described in EcoCyc (Keseler et al., 2009); a schematic of the resulting model is shown in Fig. 1. Glucose is taken up by cells and broken down to acetyl-CoA by the glycolysis pathway at a rate v_1, producing 12 ATP molecules (including the yield from coenzyme reduction) and 2 acetyl-CoA molecules per glucose molecule. Acetyl-CoA is converted to acetate and excreted from the cell at a rate v_2, producing one additional ATP molecule per acetyl-CoA molecule. Acetate in the medium is taken up by cells and converted to

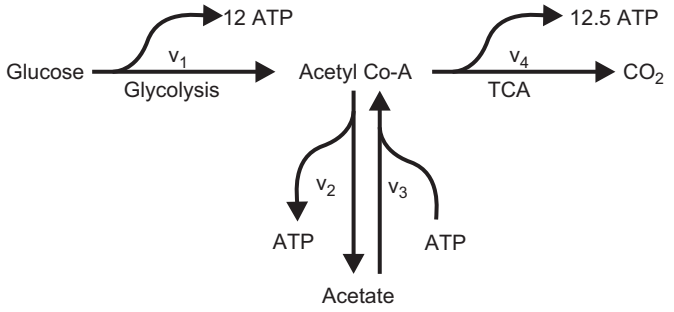

Fig. 1. Schematic of *E. coli* central metabolism. Glycolysis converts glucose into acetyl coenzyme A at rate v_1, producing 12 ATP and 2 acetyl Co-A per glucose molecule. Acetyl Co-A is converted to acetate and excreted from the cell at rate v_2, producing 1 ATP. Acetate is taken up by the cell and converted to acetyl Co-A at rate v_3, consuming 1 ATP. The TCA cycle reduces acetyl Co-A to CO_2 at rate v_4, producing approximately 12.5 ATP per acetyl co-A molecule (we assume this as constant). See Table 1 for rate equations.

acetyl-CoA at a rate v_3, and this reaction consumes one ATP molecule per acetate molecule. Intracellular acetyl-CoA is reduced to carbon dioxide by the TCA cycle, which occurs at a rate v_4 and produces 12.5 ATP molecules per acetyl-CoA molecule (again including the yield from coenzyme reduction). The number of ATP molecules produced by the TCA pathway actually depends on intracellular conditions but is assumed constant for simplicity. Given the stoichiometry of *E. coli* metabolism as well as the metabolic rates v_1–v_4, the growth of *E. coli* in a medium consisting of glucose and acetate can be described by the following system of differential equations:

$$\frac{d[\mathrm{Glu}]}{dt} = -v_1 \cdot n(t)\frac{V_c}{V_m} \tag{1}$$

$$\frac{d[\mathrm{AcCoA}]}{dt} = 2v_1 - v_2 + v_3 - v_4 \tag{2}$$

$$\frac{d[\mathrm{Ace}]}{dt} = (v_2 - v_3)n(t)\frac{V_c}{V_m} \tag{3}$$

$$\frac{dn}{dt} = n(t)\cdot V_c(12v_1 + v_2 - v_3 + 12.5v_4)g \tag{4}$$

Here [Glu] and [Ace] are the concentrations of glucose and acetate in the medium, [AcCoA] is the concentration of acetyl coenzyme-A within the cells, $n(t)$ is the number of bacteria in the population, V_c is cell volume (2×10^{-15} L; Mengin-Lecreulx et al., 1982), and V_m is the volume of the medium (0.01 L). The rates v_1–v_4 (see next paragraph) are in units of mM/min within a bacterial cell. Thus, the rates of change in [Glu] and [Ace] are scaled by the factor V_c/V_m, which scales the impact of each cell to the larger volume of the medium, and $n(t)$, the number of cells. These terms are unnecessary for [AcCoA], since this in an intracellular concentration. The conversion constant g in Eq. (4) describes the efficiency with which ATP is converted into bacterial cells (2×10^9 cells mmol^{-1}), which was assumed to be constant (Bauchop and Elsden, 1960; Varma et al., 1993). Initial concentrations of glucose (1.39 mM) and acetate (9.72 mM) in the medium were from Le Gac et al. (2008), and the intracellular concentration of acetyl coenzyme-A (0.395 mM) was the average of several estimates (Bennett et al., 2009; Buchholz et al., 2001; Hiller et al., 2007; Walsh and Koshland, 1985). The initial population size was 10^8 cells, and the system of differential equations was numerically solved for a time period of 24 h, the time period between transfers in the batch cultures of Friesen et al. (2004), Tyerman et al. (2005) and Le Gac et al. (2008).

The rates v_1–v_4 of the metabolic pathways in Eqs. (1)–(4) depend on the concentrations of glucose, acetate, and acetyl-CoA,

Table 1
Pathways in the model. x(Glu)=glycolysis/decarboxylation expression as a function of glucose concentration (dimensionless); y(Glu)=AcCoA synthase/TCA expression as a function of glucose concentration (dimensionless); $v_{i\max}$=maximum rate of pathway i (mM/min); $K_{mi,j}$=half-saturation constant of metabolite j for pathway i (mM); and square brackets refer to the concentration (mM) of the metabolite within. Glu=glucose, AcCoA=acetyl co-enzyme A, pta=phosphotransacetylase, ackA=acetate kinase, Ace=acetate.

Pathway	Rate	Parameters
Glycolysis	$v_1 = \frac{x(\mathrm{Glu})\,v_{1\max}[\mathrm{Glu}]}{1+([\mathrm{Glu}]/K_{m1,\mathrm{Glu}})+([\mathrm{AcCoA}]/K_{m1,\mathrm{AcCoA}})}$	$v_{1\max}=146.6$ $K_{m1,\mathrm{Glu}}=0.04$ $K_{m1,\mathrm{AcCoA}}=7.6$
pta/ackA	$v_2 = \frac{x(\mathrm{Glu})\,v_{2\max}[\mathrm{AcCoA}]}{K_{m2,\mathrm{AcCoA}}+[\mathrm{AcCoA}]}$	$v_{2\max}=300$ $K_{m2,\mathrm{AcCoA}}=15$
AcCoA synthase	$v_3 = \frac{y(\mathrm{Glu})\,v_{3\max}[\mathrm{Ace}]}{K_{m3,\mathrm{Ace}}+[\mathrm{Ace}]}$	$v_{3\max}=50$ $K_{m3,\mathrm{Ace}}=0.07$
TCA	$v_4 = \frac{y(\mathrm{Glu})\,v_{4\max}[\mathrm{AcCoA}]}{K_{m4,\mathrm{AcCoA}}+[\mathrm{AcCoA}]}$	$v_{4\max}=50$ $K_{m4,\mathrm{AcCoA}}=0.05$

as well as on the expression levels of the relevant enzymes, as described in Table 1. Published estimates of maximum rates and half-saturation constants differ among studies, often by an order of magnitude or more, and so these parameters were chosen to yield growth curves similar to those observed in the conditions we modeled. The concentrations of substrates and products constitute the ecological environment, the state of which is itself influenced by the metabolic rates, since these determine the change in substrate and product concentrations.

Crucially, the metabolic rates v_1–v_4 are also determined by the phenotype of the cell, i.e., by the expression levels of the relevant enzymes. We assumed that the metabolic rates were proportional to these expression levels and that the expression level of glycolysis and acetate secretion is given by a function x[Glu] of the glucose concentration. The reaction norm x[Glu] lies in the interval [0,1] and scales the metabolic rates v_1 and v_2 as described in Table 1. At the same time, the expression level of the acetate metabolism (acetate uptake and TCA cycle) is described by a function y[Glu], which also has values in the interval [0,1] and scales the metabolic rates v_3 and v_4 as described in Table 1.

The reaction norms x[Glu] and y[Glu] are phenotypic properties of a cell, and to study their evolution, we assume a basic trade-off between glycolysis expression and TCA expression. Specifically, we assume that

$$y[\mathrm{Glu}] = 1 - x[\mathrm{Glu}]^a \tag{5}$$

where a is a parameter that describes the curvature of the trade-off. This relationship is always monotonically declining, but it can be convex (positive second derivative, $a<1$), linear ($a=1$), or concave (negative second derivative, $a>1$) (Fig. 2C). As a consequence of this trade-off, for any given glucose concentration the reaction norm x[Glu] determines the levels of expression of all relevant pathways (Table 1).

The reaction norm x[Glu] represents a plastic response to glucose concentration and describes how glycolysis expression changes over the course of each growth period as glucose is consumed by the bacteria. To facilitate modeling the evolution of this reaction norm, we assumed that x[Glu] is a sigmoidal function of the glucose concentration

$$x[\mathrm{Glu}] = \frac{e^{r([\mathrm{Glu}]-s)}}{1+e^{r([\mathrm{Glu}]-s)}} \tag{6}$$

The quantities s and r in this expression control the shape of the reaction norm of gycolysis expression to glucose concentration (Fig. 2A, B). These quantities are the phenotypic traits whose evolutionary dynamics we address in the next section. In particular, we are interested in determining the evolutionary dynamic of the trait s, which determines the position of the reaction norm

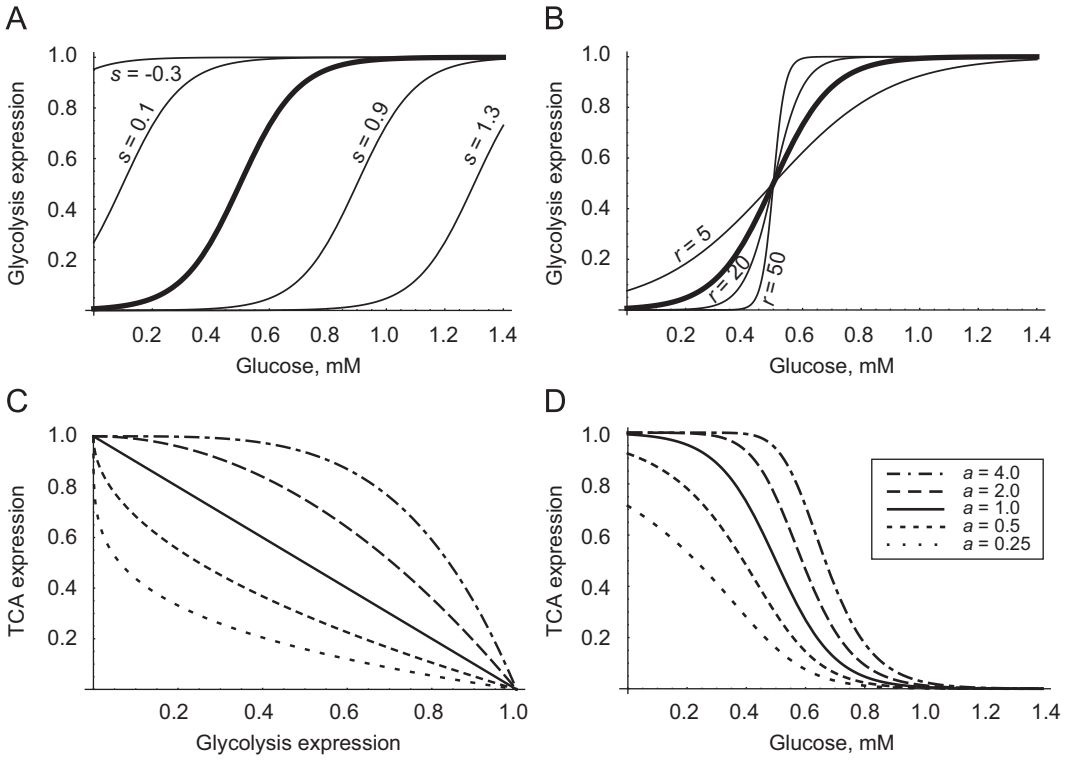

Fig. 2. Representative reaction norms and trade-off curves. The boldface curves in A and B represent the same set of parameter values ($r=10$, $s=0.5$). (A) Reaction norms of glycolysis expression for different values of s, the shift from left to right ($r=10$); (B) reaction norms of glycolysis expression for different values of r, the steepness of the reaction norm ($s=0.5$); (C) trade-off between glycolysis expression and TCA expression for different values of a, the trade-off curvature; and (D) reaction norms of TCA expression for different values of a ($r=10$, $s=0.5$).

x[Glu], and hence the degree of specialization on the different substrates: decreasing s shifts the reaction norm to the left, i.e., toward glycolysis specialization, whereas increasing s shifts the reaction norm to the right, i.e., toward TCA specialization (Fig. 2A). More precisely, as glucose concentration declines over the course of a growth period, a high value of s leads to a relatively early start to the decline in glycolysis expression (and the corresponding increase in TCA expression), whereas lower values of s lead to a late onset of glycolysis decline. Mathematically, $s>0$ describes the glucose concentration at which glycolysis expression is half of its maximum value. The effect of the parameter r is to change the steepness of the change in expression; as r becomes large, x[Glu] approaches a switching function (Fig. 2B). The effect of the trade-off curvature (Eq. (5)) on the shape of the TCA reaction norm is shown in Fig. 2D.

2.2. Evolutionary model

Given the assumptions of the model, bacterial growth is completely determined by the level of glycolysis expression, x[Glu], and the concentrations of glucose and acetate in the medium. The concentrations of these nutrients are, in turn, determined by the metabolic activity of the resident bacteria. The evolution of such a system, in which the phenotypic composition of the population is an important component of the environment, can be well represented in the modeling framework of adaptive dynamics (Dieckmann and Law, 1996; Geritz et al., 1998; Metz et al., 1996). Adaptive dynamics assumes that reproduction is clonal, that ecological and evolutionary timescales are separate (i.e. that evolution is mutation limited), that mutations are of small phenotypic effect, and that mutants appear at low initial frequency (Geritz et al., 1998; Metz et al., 1996). The last of these assumptions allows the important simplification that the effect of newly arising mutants on the selective regime is negligible.

We used the framework of adaptive dynamics to analyze the evolutionary dynamics resulting from our model for s (shift of the reaction norm left or right). As described above, mutants were assumed to have negligible effect on the growth environment (i.e., only the resident phenotype contributed to changes in glucose and acetate concentrations). Thus, although the relevant environmental factors fluctuate over a 24 h cycle, their levels at any given point during the growth cycle are completely determined by the resident bacterial phenotype. For residents with low s (i.e. relative glucose specialists), the concentration of glucose declines relatively quickly, while the acetate concentration initially increases, declining only once glucose is depleted. For residents with higher values of s (relative acetate specialists), glucose concentration declines more slowly and is never fully depleted, while acetate concentration begins to decline sooner after a smaller initial increase.

Although r (steepness of the reaction norm) is also potentially subject to selection, for simplicity we held r constant in these analyses. Solutions in which r and s were allowed to vary independently (described below) showed that r is subject to directional selection for increasing values. Since the maximum rate of change in expression is likely to be constrained by a physiological limit, this directional selection suggests that r is likely to be fixed at or near this limit (whatever it is). Therefore, it is reasonable to study the evolution of the phenotype s for various fixed values of r.

We visualized the resulting evolutionary dynamics using pairwise invasibility plots (PIPs; Geritz et al., 1998; van Tienderen and de Jong, 1986). These plots map the fate of possible mutant phenotypes (on the y-axis) appearing at low initial frequency in different resident populations (on the x-axis). The plots are filled (gray) for areas in this 2-dimensional phenotype

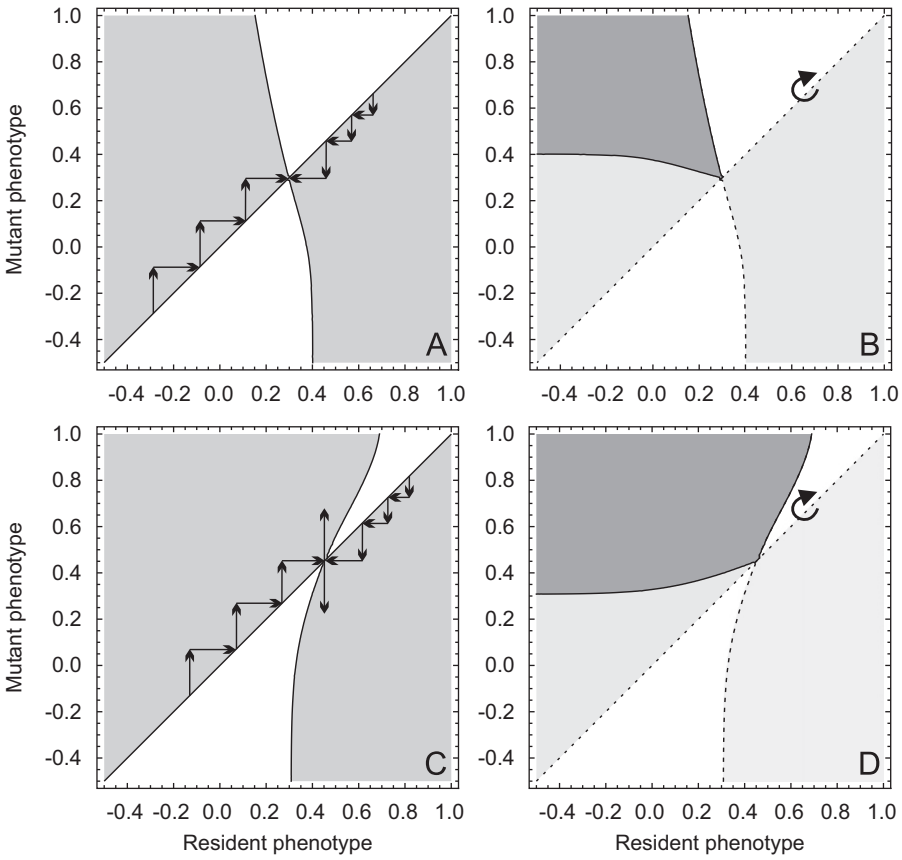

Fig. 3. Representative pairwise invasion plots for the two classes of dynamics occurring in the model. Black lines represent the zero contours of invasion fitness, the borders between regions of phenotype space in which mutants can (gray) and cannot (white) invade. In both situations, the evolutionarily singular strategy (the intersection of the zero contour with the 45°-line) is convergence stable: a monomorphic population evolving through small changes will converge to this point from either a higher or a lower phenotypic value. (A) The evolutionarily singular strategy is also an evolutionarily stable strategy (ESS). Mutants closer to the ESS invade (vertical arrows) and replace the resident population (horizontal arrows); once at the ESS, mutants with higher and lower phenotypic values have negative invasion fitness, (B) the region of mutual invasibility (dark gray) is the intersection of the region of positive invasion fitness with its reflection about the 45°-line. In the case of an ESS, this region is not accessible by a small mutation from the ESS, (C) the evolutionarily singular strategy is a branching point. The population converges to the singular point as in the ESS case, but once there mutants with higher and lower phenotypic values have positive invasion fitness, and (D) the region of mutual invasibility in the case of a branching point; in this case this region is accessible by small mutations from the singular point. See Geritz et al. (1998) for a more complete discussion of the possible configurations of PIPs and their corresponding evolutionary outcomes.

space in which the invasion fitness is positive, i.e. in which the mutant can increase from low initial frequency. In our plots, mutants with positive invasion fitness were those that increased in frequency over a 24 h growth period. (Supplement A: Mathematica notebook for *s* PIPs)

The zero contour of the invasion fitness function separates areas in which the mutant can potentially invade from those in which it is doomed to extinction. The evolutionary dynamics of the population can be inferred from the intersection of the zero contour of the invasion fitness function with the 45° line (see Fig. 3). This point represents an "evolutionarily singular strategy" (Geritz et al., 1998), at which the local fitness gradient is zero (i.e. there is no directional selection). Depending upon the configuration of invasion fitnesses near this intersection, the singular strategy may represent an evolutionary attractor, toward which monomorphic populations with higher and lower phenotypic values will converge, or a repeller, from which a monomorphic population will evolve further away. Further, in the case of an attractor, different configurations indicate the existence of either an evolutionarily stable strategy (ESS), in which case the population remains monomorphic, or a branching point, in which case the population becomes dimorphic, with two phenotypes diverging in opposite directions from the singular point. See Fig. 3 and Geritz et al. (1998) for examples of ESS and evolutionary branching configurations.

We also modeled evolutionary dynamics in which *r* was treated as an evolving trait, and *r* and *s* were allowed to vary independently. In this case, we calculated one-dimensional selective gradients for each trait by comparing invasion fitnesses at two nearby trait values and dividing by the difference in trait values. The two-dimensional selective gradient at each point in trait space was calculated as a Euclidian vector of the two fitness differences. (Supplement B: Mathematica notebook for two trait streamplots).

Examination of PIPs also allows identification of regions of phenotype space in which each of two phenotypes can invade a resident population comprised of the other, i.e. regions of mutual invasibility (see Fig. 3B, D). Mutual invasibility occurs for a pair of phenotypes if each has positive invasion fitness in a population where the other is resident; in the PIPs this is evident when the positive regions of the PIP and its reflection about the 45° line overlap (see Fig. 3B, D). In these regions, coexistence is possible on ecological time scales due to negative frequency dependence: each phenotype increases in relative frequency when rare, so neither can take over the population. When the singular point is a branching point, the region of coexistence is accessible from the singular point, and two phenotypes can potentially coexist on an evolutionary time scale. In the case of an ESS, the region of coexistence is not accessible from the singular point via small mutations, and only transient polymorphisms are possible.

While PIPs concisely represent the evolutionary dynamics of a monomorphic population, they do not describe the continued evolution of a population that has become dimorphic through evolutionary branching. To explore the evolutionary dynamics of s within the region of mutual invasibility, we modeled the growth of two resident phenotypes using iterated numerical simulations, with growth of both residents feeding back onto the growth environment. To do so, we calculated equilibrium frequencies by iterating the demographic model over a number of 24 h growth periods. At the end of each growth period, the densities of both residents were reduced 100-fold and the concentrations of glucose and acetate reset to their original levels (to simulate transferring 100 μL of culture to 10 mL of fresh medium). Simulated growth periods and transfers were iterated until the relative frequencies of the two resident phenotypes stabilized, assumed to have occurred when the change in relative frequency from one growth period to the next fell below 10^{-6}. As for the two-trait simulations above, we calculated one-dimensional selective gradients for each resident phenotype by comparing invasion fitnesses at two nearby trait values and dividing by the difference in trait values. The two-dimensional selective gradient for each pair of trait values was calculated as a Euclidian vector of the two fitness differences. (Supplement C: Mathematica notebook of two-resident simulations).

We represented the selective gradients of two residents within the region of mutual invasibility, and the corresponding expected evolutionary trajectories, using stream plots. If the trajectories represented in these plots converge to a point within the region of mutual invasibility, this point is an evolutionarily singular coalition, at which the local fitness gradients for both residents are zero (Geritz et al., 1998). As in the monomorphic case, an evolutionarily singular coalition may or may not be ESS stable. If both phenotypes are fitness maxima, the singular coalition is ESS stable and cannot be invaded; in this case the dimorphic population is expected to persist (Geritz et al., 1998). If one or both phenotypes are fitness minima, nearby phenotypes can again invade, and further evolutionary branching is expected (Geritz et al., 1998).

3. Results

The kinetic model yielded population growth curves that were qualitatively similar to those obtained in the evolution experiment for some combinations of parameters (Fig. 4; cf. with Fig. 1 of Le Gac et al., 2008). Growth of phenotypes other than glucose specialists was diauxic, with rapid growth until glucose was depleted and slower growth thereafter.

The evolutionary dynamics of s, the shift from left to right of the reaction norm, fall into one of two classes (representatives of both classes are shown in Fig. 5). In both cases, an evolutionarily singular strategy exists that is convergence stable, i.e. for which the local fitness gradients for nearby phenotypes lead to the singular point (Fig. 5). This point is an evolutionary attractor, to which monomorphic populations are expected to converge whether they start with a higher or a lower value of s.

Once the population has reached the evolutionary attractor, subsequent evolutionary behavior depends upon the steepness of the reaction norm (r) and the convexity of the trade-off (a). For concave, linear, and slightly convex trade-offs (sufficiently large a), and for shallow reaction norms (sufficiently small r), the singular strategy is also an evolutionarily stable strategy (ESS), a phenotype that cannot be invaded by a mutant with a similar phenotype (Maynard Smith, 1982). In this case, the population evolves to the ESS and remains monomorphic. The value to which

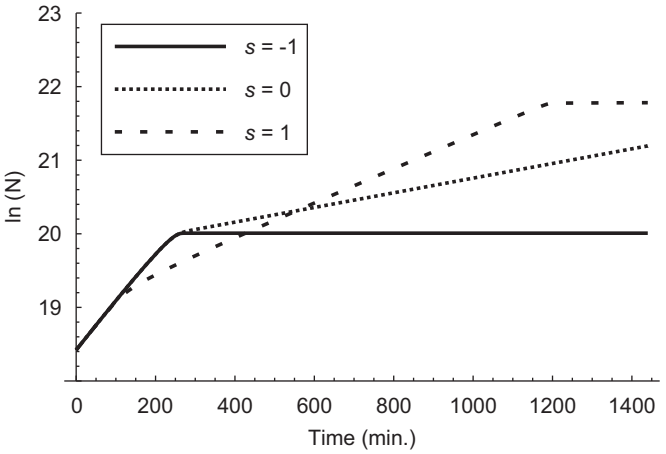

Fig. 4. Growth curves for glucose specialist ($s=-1$), generalist ($s=0$), and acetate specialist ($s=1$) phenotypes growing in isolation. The following parameters were used to generate these growth curves: $a=1$, $r=20$, and initial population size$=10^8$ cells.

s converges when the singular point is an ESS is between 0 and 0.5 (Fig. 5 D, G–I).

For sufficiently convex trade-offs (small a) and steep reaction norms (large r), the singular point is convergence stable but is not an ESS, i.e. the singular point is at a fitness minimum. In this case, mutant phenotypes with higher and lower values than that of the resident have positive invasion fitness, and s undergoes evolutionary branching (Fig. 5A–C, E, F).

For the combinations of parameters we tested, the trends described above (ESS for large values of a and small values of r) always held. That is, for a given value of a, a value of r exists above which the singular strategy is, and below which it is not, an ESS. Similarly, for a given value of r, a value of a exists below which the singular strategy is, and above which it is not, an ESS. While our sampling of the parameter space was necessarily incomplete, these trends hold at least for $0.1 \le a \le 2.0$ (sampled in steps of 0.1) and $2 \le r \le 20$ (sampled in steps of 2). For $a > 2.0$ and $r > 20$, our sampling was much less dense, but up to very large (probably biologically unrealistic) values, the PIPs change little with further increases of a and r. Because we sampled hundreds of combinations of the parameters a and r, and because additional PIPs would provide little additional information, we have shown only a representative sample of the PIPs we generated in Fig. 5.

In some cases (e.g. Fig. 5C) a second singular point exists at a negative trait value; this point is an evolutionary repeller, meaning that populations with trait values below the singular point will evolve to still lower values of s. In the context of the model, this means that populations specialized on glycolysis will evolve to become slightly more specialized. However, for these trait values the reaction norms are nearly flat for all positive glucose concentrations (e.g., Fig. 2A, $s=-0.3$), so evolution to still lower values of s (shifting the reaction norms further left) has very little impact on expressed phenotypes. As a result, the selective gradients in the vicinity of the repellers are so small (on the order of 10^{-13}) that they are only relevant for very large populations, and so we do not discuss them further.

Mutual invasibility, in which each of two phenotypes has positive invasion fitness when the other phenotype is resident, occurs in a large region of trait space. In the cases in which an ESS exists, the region of mutual invasibility is not accessible from the singular point. Before the population reaches the singular point, though, mutation may carry a population into this region, and thus it is worth considering the resulting evolutionary dynamics. Stream plots of selective gradients for two residents show that

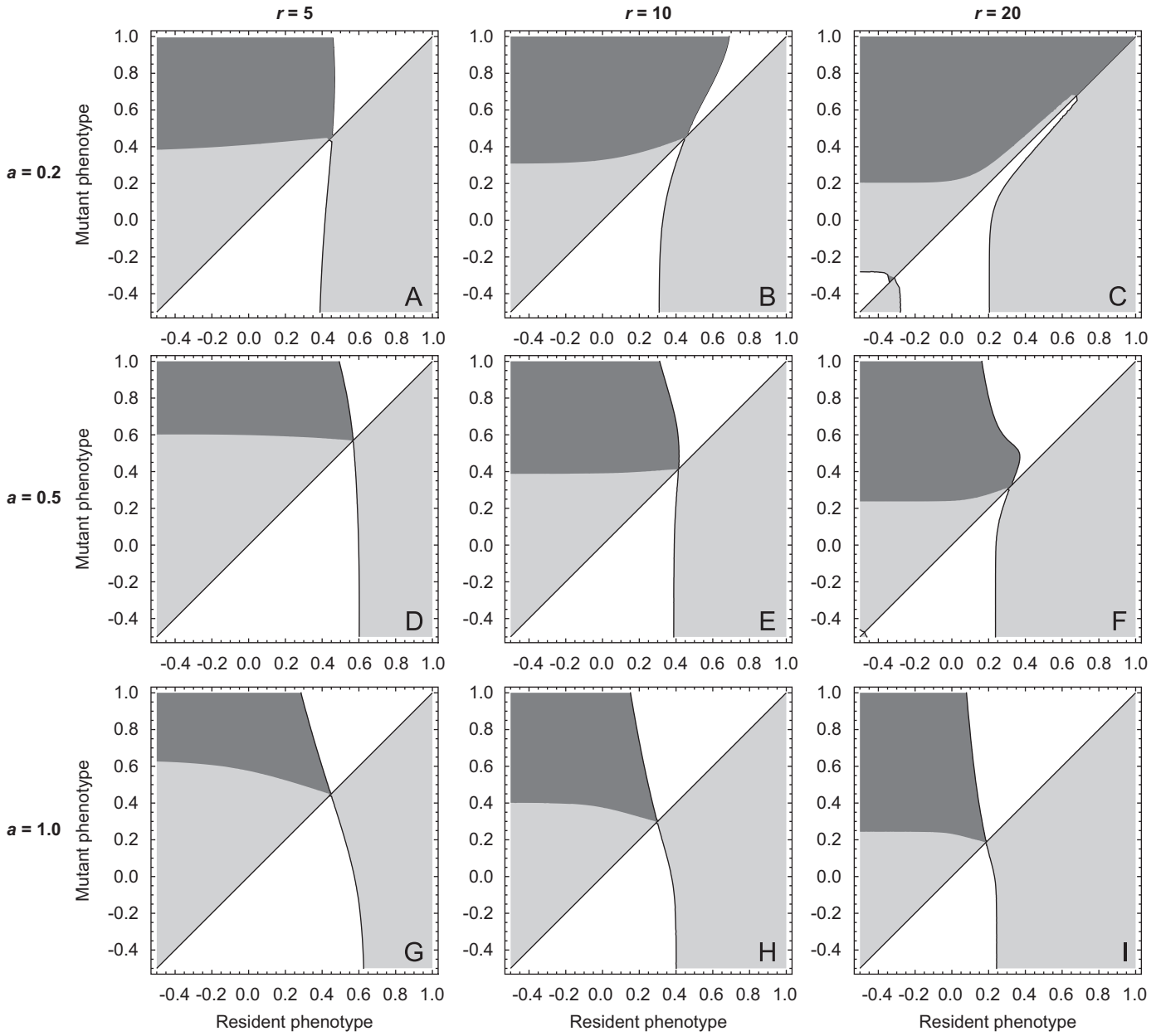

Fig. 5. Pairwise invasion plots for s, the shift from left to right of the reaction norm, for different values of r (steepness of the reaction norm) and a (convexity/concavity of the trade-off curve). Dark shading indicates the region of mutual invasibility. In plots A, B, C, E, and F, the evolutionarily singular strategy is a branching point; in D, G, H, and I, it is an ESS. Some jaggedness exists due to artifacts of numerical approximation.

only transient coexistence is possible in these cases, as the adaptive dynamics lead out of the region of coexistence (Fig. 6A, C–D). In cases in which evolutionary branching occurs, stream plots of selective gradients often show convergence to a point within the region of mutual invasibility (e.g. Fig. 6B), indicating that at least two different trait values can coexist on an evolutionary time scale. In some of these cases the evolutionarily singular coalition is evolutionarily stable (both phenotypes are fitness maxima); in other cases one or both of the phenotypes is a fitness minimum, i.e. a branching point (Table 2).

The selective gradients when s and r were allowed to vary independently show stabilizing selection for a small, positive value of s ($s \cong 0.5$), and directional selection for increasing values of r (Fig. 7). Higher resolution plots (not shown) reveal that selection for increasing r continues, but declines in magnitude, at least up to moderately high values ($r \geq 20$). Thus, r evolves to values at which evolutionary branching may occur in s if the trade-off between glycolysis expression and TCA expression is sufficiently convex. At large values of r, the reaction norm approaches a switching function, and further increases in r have little effect on either the shape of the reaction norm or the resulting dynamics of s.

4. Discussion

Our results describe an evolutionary pathway leading to metabolic diversification in a sympatric environment without spatial structure. For some combinations of parameters (steep reaction norms and convex trade-offs), evolutionary branching leads to stable coexistence of at least two distinct metabolic phenotypes. This diversification occurs in an environment that fluctuates predictably over a wide range of the relevant condition (the daily cycle of high to low glucose concentration), which

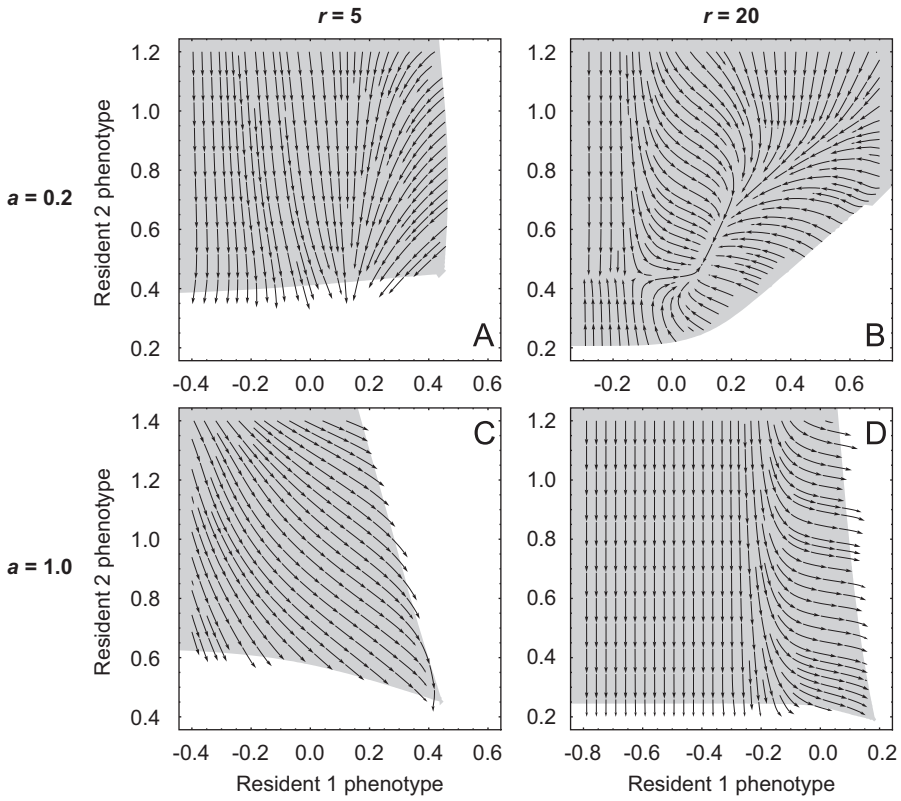

Fig. 6. Selective gradients for two resident phenotypes at different values of r (steepness of the reaction norm) and a (convexity/concavity of the trade-off curve). Shading (gray) indicates the region of mutual invasibility.

Table 2
Evolutionarily singular coalitions for selected combinations of the parameters a (convexity/concavity of the trade-off curve) and r (steepness of the reaction norm). "↑" and "↓" indicate fitness maxima and minima, respectively.

a	r	Resident 1		Resident 2	
		s		s	
0.2	15	0.0920	↓	0.5010	↓
0.2	20	0.1020	↓	0.4850	↓
0.3	10	0.0780	↓	0.4740	↑
0.3	15	0.1212	↓	0.4702	↓
0.3	20	0.1190	↓	0.4366	↓
0.4	15	0.1220	↓	0.4220	↑
0.4	20	0.1234	↓	0.3834	↓
0.5	15	0.1380	↑	0.3700	↑
0.5	20	0.1205	↑	0.3290	↑

makes the reduction of plasticity (specialization) that occurs in one type particularly surprising. Individual bacteria live their entire lives in a subset of the total range of conditions, and so an ideal strategy would seem to be a highly plastic one.

Diversification in this case occurs through gradual shifting of reaction norms. For ranges of parameter values at which two phenotypes can coexist, stable values of s tend to be around $s=0.1$ and 0.5. A phenotype of $s\approx 0.5$ is a generalist, capable of achieving maximal expression levels of both pathways when the trade-off curve is concave, linear, or slightly convex. For sufficiently convex trade-offs, high levels of TCA expression become unattainable for this phenotype. A phenotype of $s\approx 0.1$ is a glycolysis specialist, for which the glycolysis pathway is always expressed at some level, and TCA is always down regulated for all but very concave trade-offs. Emergence of these phenotypes is qualitatively consistent with the ecological character displacement observed in the evolutionary experiment of Tyerman et al. (2008), in which the FS type is a metabolic generalist and SS a glycolysis specialist.

Evolutionary branching in this system can be understood as a change in the available niches, as evolutionary change in the resident population changes the time course of the daily fluctuation in nutrient concentrations. For example, as s evolves to lower values (higher glycolysis expression), more acetate is produced early in the growth cycle. Greater availability of acetate opens up a niche for a high s phenotype (higher TCA expression). If a high s mutant appears and begins to increase in frequency, more glucose will be available later in the growth cycle, leading to selection for further decreases in s in the low s resident. This situation creates a positive feedback loop: as each phenotype evolves away from the other, it creates a selective pressure on the other phenotype to evolve still further away.

The specialization on glucose in the SS type is due to a reduction in plasticity: the glycolysis pathway, initially induced by the presence of glucose, has become constitutively expressed, so that it is no longer dependent on the original environmental condition (glucose). Reduced plasticity in this case results not from any change in the shape of the reaction norm, but rather from shifting the entire curve to the left (Fig. 2A). Plasticity is effectively reduced when part of the reaction norm is shifted outside of the range of environmental conditions (glucose concentrations) in the experiment. Still larger shifts would result in fixation of one pathway or the other, as the phenotype (expression level) is essentially zero or one throughout this range.

Similar patterns of reduced phenotypic plasticity have often been interpreted as evidence for genetic assimilation (e.g. Aubret and Shine, 2009; Ledon-Rettig et al., 2008; Palmer, 2004; West-Eberhard, 2003), a process in which natural selection causes a phenotype that is initially induced by an environmental stimulus to become constitutively expressed, so that the original stimulus is no longer required for its expression (Waddington, 1953; Waddington, 1961).

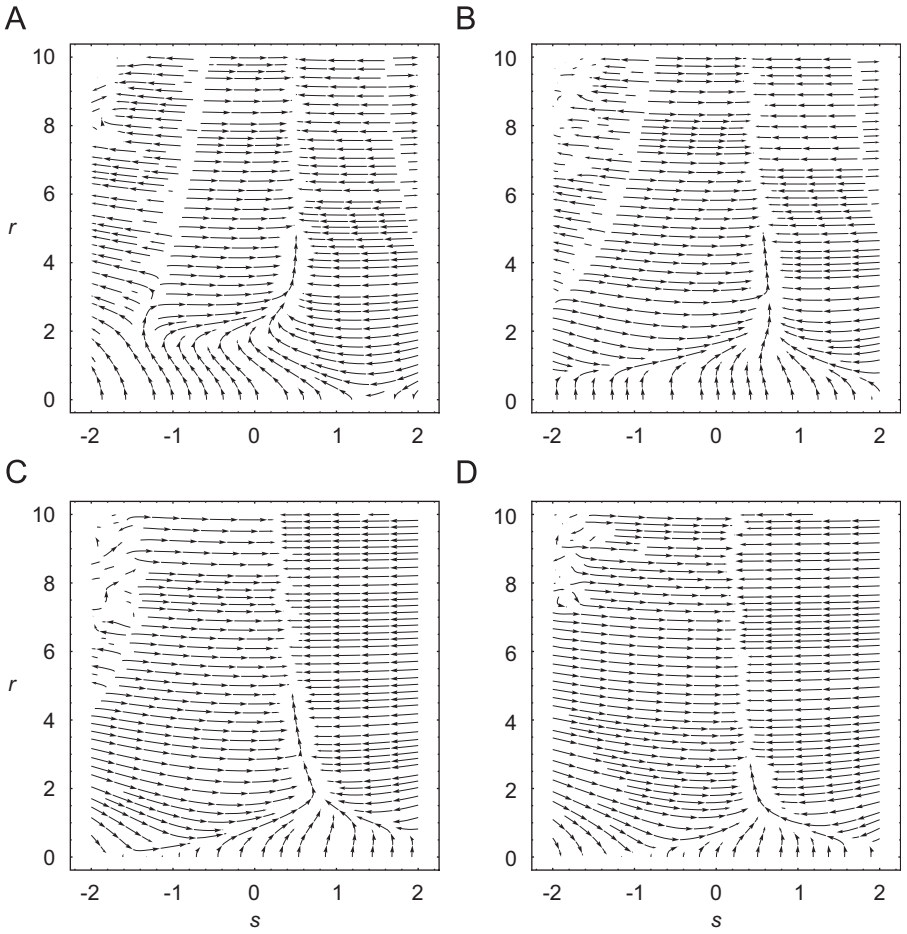

Fig. 7. Selective gradients for r and s varying independently at different values of a (convexity/concavity of the trade-off curve). (A) $a=0.25$, (B) $a=0.5$, (C) $a=1.0$, and (D) $a=2.0$.

However, the pattern of reduced plasticity is not sufficient to conclude that the process of genetic assimilation is the cause. In most conceptions of genetic assimilation, an important component is the "phenotype first" aspect (also known as "plasticity first" or "genes as followers"), meaning that the phenotype in question first appears due to environmental change, rather than genetic change (Hall, 2001; Price et al., 2003; Schwander and Leimar, 2011; West-Eberhard, 2003; West-Eberhard, 2005). In this view, it is the environmentally induced change (plastic response) that moves the population within the range of attraction of a new adaptive peak, effectively altering the direction of selection (Price et al., 2003). It is not immediately obvious how these concepts, which are most often considered in terms of discrete changes, can be reflected in a conceptual framework (adaptive dynamics) that has gradual change as a basic assumption and in which relevant aspects of the environment are determined by the phenotypes that are currently present in the population. In our model, the phenotypes, their relative frequencies, and the resulting environment change gradually, and diverging phenotypes coevolve in response to these changes. It is thus difficult to say whether or not the "phenotype first" requirement can be met and whether or not the concept of genetic assimilation is relevant to this model.

Our results show that diversification and coexistence are strongly dependent on the shape of the trade-off between expression of the glycolysis and acetate excretion pathways and that of the acetate uptake and TCA pathways. In the most literal sense, a linear trade-off implies that the total expression of these pathways is constant, so that an increase in one is exactly offset by an equivalent decrease in the other. For the convex and concave cases, the total expression is lower or higher, respectively, when both pathways are active than when one is fully up regulated and the other shut down. Because the effect of expression on growth depends on a complicated feedback of phenotype, metabolism, and environment, the shape of the trade-off curve does not easily translate into terms with a direct relevance to fitness. To gain an intuitive sense of this relationship, though, we can think of a concave trade-off curve as one in which intermediate phenotypes are favored (perhaps because of a synergy between the two pathways) and a convex trade-off as one in which extreme phenotypes are favored (perhaps because some intermediate metabolite of one pathway interferes with the expression of the other). In this sense, the metabolic diversification predicted for convex trade-offs is consistent with, for example, the inhibition of some TCA enzymes by NADH produced by glycolysis (Keseler et al., 2009).

In addition, diversification is only predicted when the value of r is relatively high (exactly how high depends upon the value of a), that is, when the reaction norm is steep. In biological terms, the effect of r is, roughly, to determine the rate at which bacteria switch from one metabolic pathway to the other ("roughly" because expression is explicitly a function of glucose concentration, and only implicitly a function of time). Depending on the values of a and s, a low value of r will often mean that one pathway or the other can never be fully upregulated, at least within the range of conditions in the model (for example, see the $s=0.1$ and 1.3 curves in Fig. 2A, the $r=5$ curve in Fig. 2B, and the $a=0.25$ and 0.5 curves in Fig. 2D). For sufficiently high r, any value of s between 0 and 1.4 allows expression arbitrarily close to

100% for both pathways, while s outside of this range amounts to complete specialization in glycolysis ($s < 0$) or TCA ($s > 1.4$).

Pfennig et al. identify as one of the "key challenges" for future research on the evolutionary effects of phenotypic plasticity to "explore parameter space over which plasticity promotes rather than impedes diversification" (Pfennig et al., 2010). Here, we have shown that, for this example at least, diversification only occurs when the trade-off between traits is sufficiently convex and the reaction norms sufficiently steep. The requirement for convex trade-offs was predicted in a different context in the covariance model of Michod (2006), in which the diversification of cell functions in a multicellular organism was predicted to occur only if the trade-off between fitness components was convex. If this principle can be generalized, it suggests that phenotypic divergence by changes in plasticity is more likely when the trade-off between performance in different environments is convex. Further, the association of diversification with steep reaction norms (high r) suggests the possibility that this sort of trait diversification is more likely for polyphenisms than for traits that vary continuously with an environmental factor. Testing these hypotheses would require traits to be measured in multiple environments, since a minimum of three measurements is required to begin to estimate or even detect curvature in a trade-off or a reaction norm.

The reduced plasticity of the SS type evolved in an environment that was both variable and predictable (the decline in glucose concentration from an initially high value in subsequent daily transfers). In our model, this reduction in phenotypic plasticity occurs in the absence of any explicit, externally imposed cost of plasticity. Rather, fitness differences emerge from the ecological conditions generated by feedback from bacterial metabolism, which is in turn based on the kinetics of metabolic pathways in individual bacteria. The only trade-off imposed is between the expression level of the glycolysis/acetate excretion pathway and that of the acetate uptake/TCA pathway. Expression level trade-offs are known to occur in *E. coli* and other bacteria because transcription factors compete for a limited pool of RNA polymerase (King et al., 2004; Nyström, 2004). Fitness effects in our model emerge from the interaction of this trade-off with the environmental feedback of the bacteria on the medium. Our results show that frequency-dependent selection can drive the evolution of specialization even when there is no inherent cost of plasticity.

Acknowledgments

MD was supported by the NSERC (Canada) and by the Human Frontier Science Program. The comments of two anonymous reviewers led to several improvements to the manuscript.

Appendix A. Supporting information

Supplementary data associated with this article can be found in the online version at doi:10.1016/j.jtbi.2011.06.007.

References

Aubret, F., Shine, R., 2009. Genetic assimilation and the postcolonization erosion of phenotypic plasticity in island tiger snakes. Curr. Biol. 19, 1932–1936.
Bauchop, T., Elsden, S.R., 1960. The growth of micro-organisms in relation to their energy supply. J. Gen. Microbiol. 23, 457–469.
Bennett, B.D., Kimball, E.H., Gao, M., Osterhout, R., Van Dien, S.J., Rabinowitz, J.D., 2009. Absolute metabolite concentrations and implied enzyme active site occupancy in *Escherichia coli*. Nat. Chem. Biol. 5, 593–599.
Buchholz, A., Takors, R., Wandrey, C., 2001. Quantification of intracellular metabolites in *Escherichia coli* K12 using liquid chromatographic-electrospray ionization tandem mass spectrometric techniques. Anal. Biochem. 295, 129–137.
de Jong, G., 2005. Evolution of phenotypic plasticity: Patterns of plasticity and the emergence of ecotypes. New Phytol. 166, 101–118.
Dieckmann, U., Law, R., 1996. The dynamical theory of coevolution: A derivation from stochastic ecological processes. J. Math. Biol. 34, 579–612.
Doebeli, M., 2002. A model for the evolutionary dynamics of cross-feeding polymorphisms in microorganisms. Popul. Ecol. 44, 59–70.
Friesen, M.L., Saxer, G., Travisano, M., Doebeli, M., 2004. Experimental evidence for sympatric ecological diversification due to frequency-dependent competition in *Escherichia coli*. Evolution 58, 245–260.
Geritz, S.A.H., Kisdi, É., Meszéna, G., Metz, J.A.J., 1998. Evolutionarily singular strategies and the adaptive growth and branching of the evolutionary tree. Evol. Ecol. 12, 35–57.
Gudelj, I., Beardmore, R.E., Arkin, S.S., MacLean, R.C., 2007. Constraints on microbial metabolism drive evolutionary diversification in homogeneous environments. J. Evol. Biol. 20, 1882–1889.
Hall, B.K., 2001. Organic selection: Proximate environmental effects on the evolution of morphology and behaviour. Biol. Philos. 16, 215–237.
Hiller, J., Franco-Lara, E., Weuster-Botz, D., 2007. Metabolic profiling of *Escherichia coli* cultivations: Evaluation of extraction and metabolite analysis procedures. Biotechnol. Lett. 29, 1169–1178.
Keseler, I.M., Bonavides-Martínez, C., Collado-Vides, J., Gama-Castro, S., Gunsalus, R.P., Johnson, D.A., Krummenacker, M., Nolan, L.M., Paley, S., Paulsen, I.T., Peralta-Gil, M., Santos-Zavaleta, A., Shearer, A.G., Karp, P.D., 2009. EcoCyc: A comprehensive view of *Escherichia coli* biology. Nucleic Acids Res. 37, D464–D470.
King, T., Ishihama, A., Kori, A., Ferenci, T., 2004. A regulatory trade-off as a source of strain variation in the species *Escherichia coli*. J. Bacteriol. 186, 5614–5620.
Kisdi, É., 2001. Long-term adaptive diversity in Levene-type models. Evol. Ecol. Res. 3, 721–727.
Le Gac, M., Brazas, M.D., Bertrand, M., Tyerman, J.G., Spencer, C.C., Hancock, R.E.W., Doebeli, M., 2008. Metabolic changes associated with adaptive diversification in *Escherichia coli*. Genetics 178, 1049–1060.
Ledon-Rettig, C., Pfennig, D., Nascone-Yoder, N., 2008. Ancestral variation and the potential for genetic accommodation in larval amphibians: Implications for the evolution of novel feeding strategies. Evol. Dev. 10, 316–325.
Maynard Smith, J., 1982. Evolution and the Theory of Games. Cambridge University Press, Cambridge.
McCairns, R.J.S., Bernatchez, L., 2010. Adaptive divergence between freshwater and marine sticklebacks: Insights into the role of phenotypic plasticity from an integrated analysis of candidate gene expression. Evolution 64, 1029–1047.
Mengin-Lecreulx, D., Flouret, B., van Heijenoort, J., 1982. Cytoplasmic steps of peptidoglycan synthesis in *Escherichia coli*. J. Bacteriol 151, 1109–1117.
Metz, J.A.J., Geritz, S.A.H., Meszèna, G., Jacobs, F.J.A., Van Heerwaarden, J., 1996. Adaptive dynamics, a geometrical study of the consequences of nearly faithful reproduction. In: van Strien, S. J., Verduyn Lunel, S. M., Eds., Stochastic and Spatial Structures of Dynamical Systems. North Holland, Amsterdam, pp. 183–231.
Michod, R.E., 2006. The group covariance effect and fitness trade-offs during evolutionary transitions in individuality. PNAS 103, 9113–9117.
Novak, M., Pfeiffer, T., Lenski, R.E., Sauer, U., Bonhoeffer, S., 2006. Experimental tests for an evolutionary trade-off between growth rate and yield in *E. coli*. Am. Nat. 168, 242–251.
Nyström, T., 2004. MicroReview: Growth versus maintenance: A trade-off dictated by RNA polymerase availability and sigma factor competition? Mol. Microbiol. 54, 855–862.
Palmer, A.R., 2004. Symmetry breaking and the evolution of development. Science 306, 828–833.
Pfeiffer, T., Bonhoeffer, S., 2004. Evolution of cross-feeding in microbial populations. Am. Nat. 163, E126–E135.
Pfennig, D.W., Wund, M.A., Snell-Rood, E.C., Cruickshank, T., Schlichting, C.D., Moczek, A.P., 2010. Phenotypic plasticity's impacts on diversification and speciation. Trends Ecol. Evol. 25, 459–467.
Price, T.D., Qvarnström, A., Irwin, D.E., 2003. The role of phenotypic plasticity in driving genetic evolution. Proc. R. Soc. B 270, 1433–1440.
Schwander, T., Leimar, O., 2011. Genes as leaders and followers in evolution. Trends Ecol. Evol. 26, 143–151.
Spencer, C.C., Bertrand, M., Travisano, M., Doebeli, M., 2007. Adaptive diversification in genes that regulate resource use in *Escherichia coli*. PLoS Genet. 3, e15.
Spencer, C.C., Tyerman, J., Bertrand, M., Doebeli, M., 2008. Adaptation increases the likelihood of diversification in an experimental bacterial lineage. PNAS 105, 1585–1589.
Tyerman, J., Havard, N., Saxer, G., Travisano, M., Doebeli, M., 2005. Unparallel diversification in bacterial microcosms. Proc. R. Soc. B 272, 1393–1398.
Tyerman, J.G., Bertrand, M., Spencer, C.C., Doebeli, M., 2008. Experimental demonstration of ecological character displacement. BMC Evol. Biol. 8, e15.
van Tienderen, P.H., de Jong, G., 1986. Sex ratio under the haystack model: Polymorphism may occur. J. Theor. Biol. 122, 69–81.
Varma, A., Boesch, B.W., Palsson, B.O., 1993. Stoichiometric interpretation of *Escherichia-coli* glucose catabolism under various oxygenation rates. Appl. Environ. Microbiol. 59, 2465–2473.
Waddington, C.H., 1953. Genetic assimilation of an acquired character. Evolution 7, 118–126.

Waddington, C.H., 1961. Genetic assimilation. Adv. Genet. 10, 257–290.
Walsh, K., Koshland Jr., D.E., 1985. Branch point control by the phosphorylation state of isocitrate dehydrogenase—a quantitative examination of fluxes during a regulatory transition. J. Biol. Chem. 260, 8430–8437.
West-Eberhard, M.J., 2003. Developmental Plasticity and Evolution. Oxford University Press, Oxford, U.K.
West-Eberhard, M.J., 2005. Developmental plasticity and the origin of species differences. PNAS 102 (Suppl), 6543–6549.
Wund, M.A., Baker, J.A., Clancy, B., Golub, J.L., Foster, S.A., 2008. A test of the "flexible stem" model of evolution: ancestral plasticity, genetic accommodation, and morphological divergence in the threespine stickleback radiation. Am. Nat. 172, 449–462.